Instrument Science Report COS 2015-06

Summary of the COS Cycle 21 Calibration Program

Hugues Sana, Andrew Fox, Julia Roman-Duval, Justin Ely, K. Azalee Bostroem, Sean Lockwood, Cristina Oliveira, Steven Penton, Charles Proffitt, David Sahnow, Paule Sonnentrucker, Jo Taylor, Alan D. Welty, Thomas Wheeler
September 25, 2015

ABSTRACT

We summarize the Cycle 21 calibration program for the Cosmic Origins Spectrograph (COS) on the Hubble Space Telescope, covering the time period from November 2013 through October 2014. We give an overview of the Calibration plan and status summaries for each of the individual proposals comprising the C21 Calibration program.

1. Introduction

The Cosmic Origins Spectrograph (COS) was installed on the Hubble Space Telescope in May 2009. Cycle 21 was thus the fifth cycle of on-orbit operations for COS, running from November 2013 through October 2014. Each cycle, the COS team monitors the performance of the COS instrument through routine calibration programs. They monitor instrument throughput, dispersion, and performance.

In this document we record and summarize the results of the 14 individual calibration programs that comprise the COS Cycle 21 calibration plan. Section 2 gives a summary and overview of the calibration plan. Cycle 21, calibration plan was composed of 10 programs monitoring calibration and instrument performance. There were two special (13523 and 13530) and 2 contingency (13532 and 135233) calibration programs in Cycle 21.

Section 3 details results from the individual calibration programs. The Appendix lists reference files produced as a result of Cycle 21 calibration programs.

2. Overview of Cycle 21 calibration programs

Table 1 summarizes the orbit allocation and usage for the regular Cycle 21 calibration programs. Cycle 21 programs are essentially continuations of the monitoring programs from the previous cycle. Reference files are updated only as-needed to maintain instrument calibration within the required specifications.

Table 1. Orbit allocation and usage during the Cycle 21 calibration programs

	External Orbits	Internal Orbits	Parallel Orbits
Allocated	38+10[C]	316+21[C]+2/HV changes	4
Executed	39	318	4
Withdrawn	0	0	0
Failed	1	0	0
Repeated	0	0	1[H,*]

[C] Contingency orbits, [H] HOPR, * One parallel orbit was repeated due to a repeat of the Prime Instrument visit (see STIS Cycle 21 ISR)

Currently available reference files can be found at the following web address: www.stsci.edu/hst/observatory/cdbs/SIfileInfo/COS/reftablequeryindex . Other products resulting from the calibration program include COS Instrument Science Reports (ISRs), COS Technical Instrument Reports (TIRs), and updates to the COS Instrument (IHB) and Data (DHB) Handbooks. Links to these documents can be found at: www.stsci.edu/hst/cos/documents . Note that TIRs are only available on the internal STScI web site. In order to retrieve TIRs a document from outside STScI, arequest needs to be sent to help@stsci.edu.

Table 2 provides a high-level summary of the calibration programs, noting specifically products and accuracy achieved. The first two columns give the Proposal ID and its title; columns 3 and 4 give the number of executed[allocated] orbits for each proposal, divided into external and internal orbits. Column 5 gives the frequency of visits for monitoring programs. Column 6 describes the resulting products. For several programs, regularly updated reference files are produced. For many others, results are either posted on the web, or simply documented in Section 3 of this report. Column 7 gives the accuracy achieved by the calibration proposal. The last column of Table 2 notes the page in this ISR on which detailed information for that program can be found.

3. Results from individual programs

The following sections summarize the purpose, status, and results from the individual calibration proposals in the Cycle 21 program.

Table 2. High-level summary of Cycle 21 calibration programs

PID	Title	Orbits used Executed [Allocated]		Frequency	Products	Accuracy Achieved	Page
		External	Internal				
NUV Monitors							
13531	**COS NUV MAMA Fold Distribution**	--	1 [1]	1/yr	Reported in this ISR	<5% on peak location of fold distribution	3
13528	**COS NUV Detector Dark Monitor**	--	52 [52]	1/week	Reported in this ISR	0.2% in global dark rate uncertainty	6
13527	**COS NUV Spectroscopic Sensitivity Monitor**	6 [6]	--	3x2/(L+M)	Reported in this ISR	S/N of 30 per resel	8
13529	**COS NUV Internal/External Wavelength Scale Monitor**	3 [3]	--	3x1	Reported in this ISR	1.7-3.7 pixels in wavelength scale accuracy	10
13526	**Monitoring of COS ACQ/IMAGE Performance**	3 [2+4^{C}]	--	2x1	None	0.5 NUV pixel	12
FUV Monitors							
13121	**COS FUV Detector Dark Monitor**	--	260 [260]	5/week	Reported in this ISR	0.1% in global dark rate uncertainty	14
13520	**COS FUV Spectroscopic Sensitivity Monitor**	23 [23+10^{C}]	--	1x/month	TDS Reference file	<2/5% relative/absolute TDS calibration	14
13522	**COS FUV Internal/External Wavelength Scale Monitor**	3 [3]	--	1/yr	Reported in this ISR	l scale accuracy: 5.7-7.5 pix G130M, 5.8-7.2 pix G160M, 7.5-12.5 pix G140L	19
13525	**COS FUV Detector Gain Maps**	--	4 [2 + 2/change]	Once per HV change	Reported in this ISR	~0.1 Pulse Height bins	21
13548	**COS observations of geo-coronal Lyman alpha emission (COS pure parallel)**	4^{P} +1^{HP}[4^{P}]	--	4x1	Reported in this ISR	N/A	22
Special Programs							
13523	**COS PtNe Lamp Cross-calibration**	--	1 [1]	1/yr	Reported in this ISR		23
13530	**COS NUV Focus Sweep**	1 [1]	--	1/yr			25
Contingency programs							
13533	**COS NUV recovery after Anomalous Shutdown**	--	0 [4^{C}]	Contingency	None	N/A	--
13532	**COS FUV Recovery After Anomalous Shutdown**	--	0 [17^{C}]	Contingency	None	N/A	--

^{C} Contingency orbits, ^{P} Parallel orbits, ^{H} HOPR

Proposal ID 13531: COS NUV MAMA Fold Distribution

(PI: Thomas Wheeler)

Analysis Lead, Others: Thomas Wheeler, Alan D. Welty (CoI)

Summary of Goals and Program Design

The performance of the NUV MAMA microchannel plate can be monitored using a MAMA fold analysis procedure that provides a measurement of the distribution of charge cloud sizes incident upon the anode giving some measure of change in the pulse-height distribution of the MCP and, therefore, MCP gain. The goal is the continued monitoring of the NUV MAMA detector and comparing the results with previous results to detect trends or anomalous behavior. This program is based on Cycle 20, Proposal 13128.

Execution : All visits were executed on May 1, 2014.

Summary of Analysis and Results

The engineering telemetry data is examined (voltages, currents, temperatures, relay positions, and status) for agreement with predicted values and previous ground and on-orbit test data. A MAMA time-tag image data is used to construct a histogram of the number of counts for each fold. The results are compared and combined with the previous test results.

Post test, a dark exposure is taken where the counters are cycled and are plotted in a histogram and compared with earlier results.

No anomalous behavior was detected. The NUV MAMA does exhibit a known high dark count rate caused by widow phosphorescence that has been increasing since installation during SMOV4. Results are sent to the COS/STIS Science Team and V. Argabright of Ball Aerospace for review and comments.

Accuracy Achieved

Position of the peak in the fold distribution can be measured to about 5% accuracy from this procedure.

Reference Files Delivered

N/A

Relevant ISRs

No ISRs will be published

Continuation Plans

This monitoring program will continue in Cycle 22 Proposal 13976. No modifications are expected.

Supporting Details:

Below is the NUV fold histogram

(**Figure 1**) followed by the post-test dark count histogram (**Figure 2**).

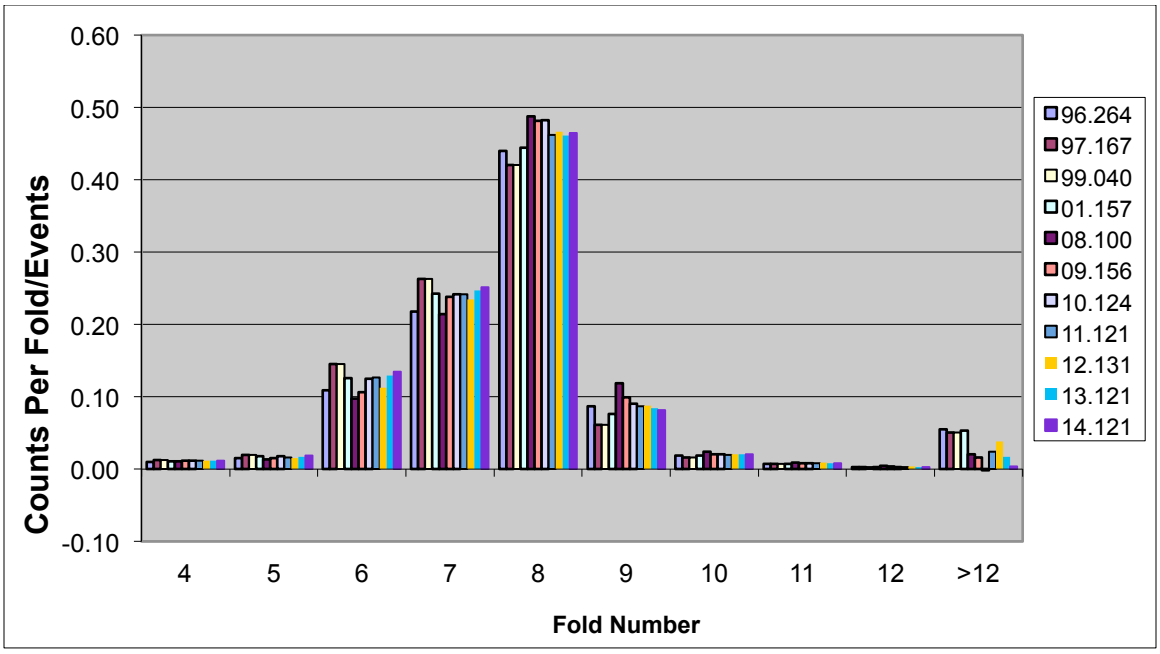

Figure 1. NUV MAMA Fold Histogram

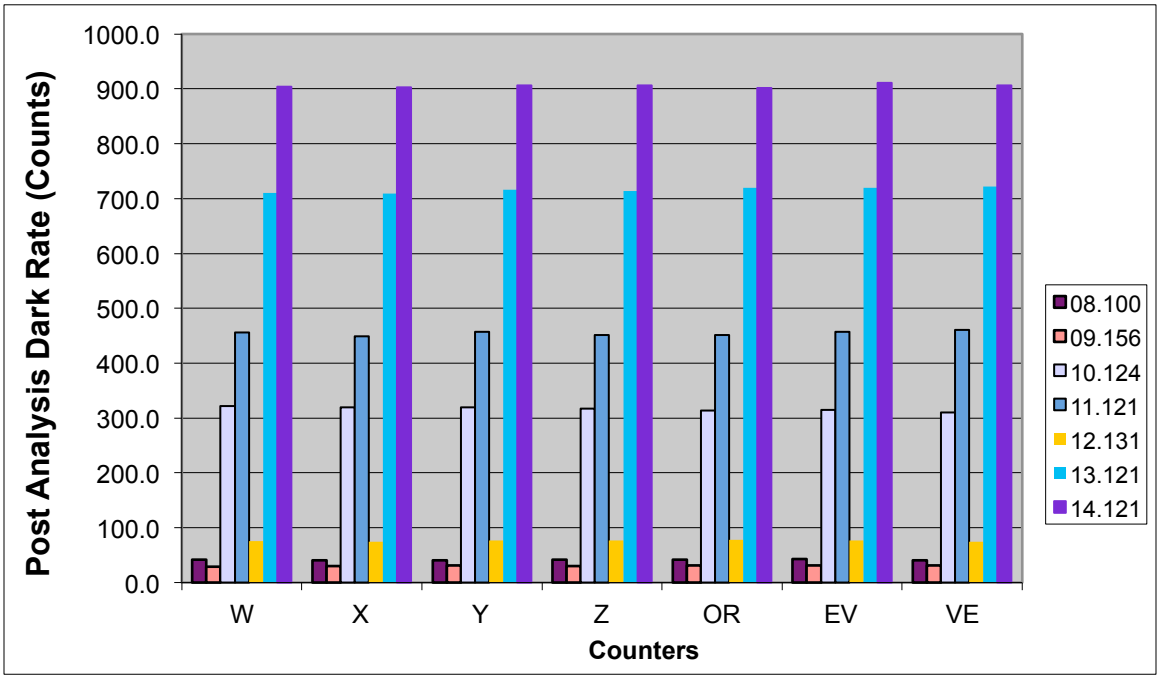

Figure 2. NUV MAMA Post-Test Dark Count Histogram

Proposal ID 13528: COS/NUV Detector Dark Monitor

(PI: Justin Ely)

Analysis Lead, Others: Justin Ely, David Sahnow, Charles Proffitt

Summary of Goals and program design

Perform routine monitoring of the NUV MAMA detector dark rate. The main purpose is to look for evidence of a change in the dark, both to track on-orbit time dependence and to check for any developing detector problems. Results from this program are used to update the ETC.

Execution

Every two weeks, two 22-minute exposures were taken with the shutter closed for a total of 52 orbits. All observations were successful.

Summary of Analysis and Results

The global dark rate of each observation was measured, and the overall trend was monitored as a function of time. The data, initially fit well with a linear relation, now shows a slower increase with time and larger variability, the latter being induced by temperature and seasonal changes (Figure 3).

Accuracy Achieved

Due to the changing trend with time, we adopt an ETC estimate for the dark-rate that corresponds to the 95% level in the probability distribution function determined from dark measurements over a period of the previous 6 months to 1 year.

Reference Files Delivered

None

Relevant ISRs

None

Continuation Plans

Program continued in Cycle 22 as 13974.

Supporting Details

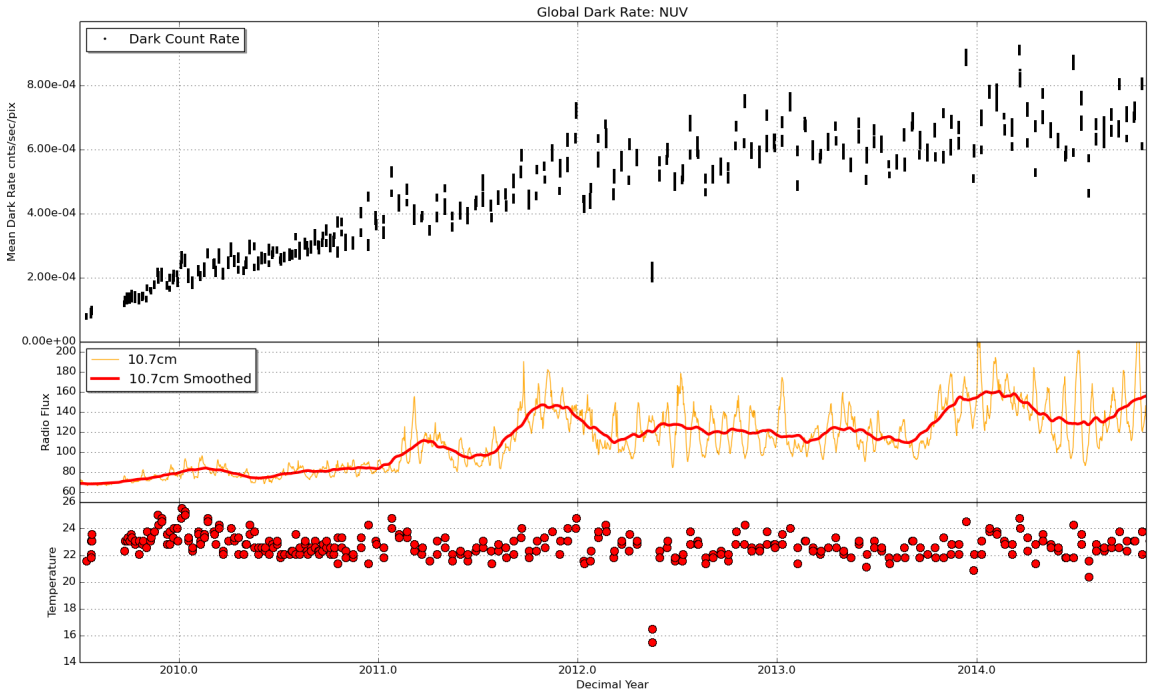

Figure 3. COS NUV dark rate as a function of time, from the COS installation through Cycle 21. The first subplot shows the measured dark-rate in 25 second increments throughout every observation. The groupings of points represent individual exposures, and demonstrate that the variability within a given exposure is low. The middle subplot displays the 10.7 cm radio flux used to track the solar cycle, and the last subplot displays the detector temperature for each observation.

Proposal ID 13527: NUV Spectroscopic Sensitivity Monitor

(PI: K. Azalee Bostroem)

Analysis Lead, Others: Jo Taylor

Summary of Goals and program design

Monitor the sensitivity of each NUV grating to detect changes due to contamination or other causes. Characterize these changes as a function of wavelength, grating, and stripe and update the time-dependent sensitivity reference file, if necessary, for use with pipeline flux calibration.

Due to sensitivity differences on the medium- and low- resolution gratings, two spectrophotometric white dwarf standard star targets are used in this monitoring: WD1057+719 for G230L, and G191B2B for G185M, G225M, and G285M.

Execution

This program was allocated 6 orbits, with two orbits executed every 4 months (Jan, Apr and Sept 2014). All visits executed nominally.

Summary of Analysis and Results

The computation of the time-dependent sensitivities for COS NUV data from previous cycles is described in Osten et al. (2010; COS ISR 2010-15) and Osten et al. (2011; COS ISR 2011-02). The same analysis techniques and code used in previous cycles are used in Cycle 21. Figure 4 summarizes the behavior of the spectroscopic sensitivity through April 2015. The G230L and G185M gratings, which have a MgF_2 coating, exhibit slightly increasing sensitivity trends with slopes between -0.2 and +1.1 %/yr. The positive trends in the G185M grating appear to have reversed in late 2011 and so these trends should be fit by a piecewise linear trend in the future. It does not appear that the trend has turned over in the G230L grating. The bare-Al gratings (G225M and G285M), which have exhibited sensitivity declines from the beginning of Cycle 17, continue to decline at a steady rate of -3.0 to -2.4 %/yr and -10.7 to -12.0%/yr respectively. These values are consistent with the results from pre-launch grating efficiency tests. The wavelength dependence of the G285M and the shortest wavelengths of G225M continues in this cycle with the same trends.

Accuracy Achieved

Phase I accuracy of S/N = 30 was achieved for G185M and G230L. The required accuracy of S/N = 30 was not achieved for G225M. The G225M/2186 setting achieved S/N = 28.3. The required accuracy of S/N = 26 in the G285M was not achieved. The G285M/2617 setting achieved S/N = 19.5 and the G285M/3094 setting achieved S/N = 19.3. However, we are currently meeting our TDS characterization requirements (2%), so that, for the time being, we do not need to increase exposure time which would lead to add additional orbit to the programs. All S/N ratios are quoted at the central wavelength and per resolution element (3 pixels).

Reference Files Delivered:

None

Relevant ISRs: None

Continuation Plans

The program continued in Cycle 21 as 13793. No changes were made.

Supporting Details

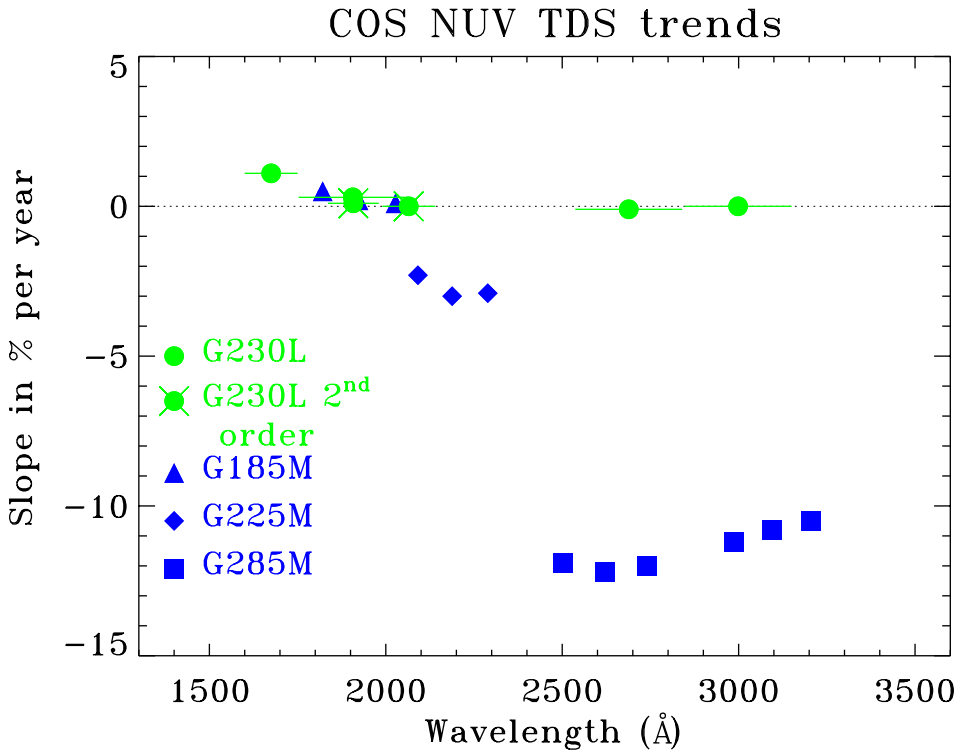

Figure 4. NUV TDS slope as a function of wavelength for different NUV gratings. Slopes are calculated based on all NUV TDS monitoring data acquired since SMOV4.

Proposal ID 13529: COS NUV Internal/External Wavelength Scale Monitor (PI: Sonnentrucker)

Analysis Lead, Others: Paule Sonnentrucker

Summary of Goals and program design
This program monitors the offset between the internal and external wavelength scales. This offset is referred to as "DELTA" in the wavelength dispersion solution reference file and corrects for the shift between the WCA and PSA in TV03 versus the shift between the WCA and PSA on orbit: (WCA - PSA)TV03 - (WCA - PSA)orbit. Analysis of TV data indicates that this DELTA (offset) is cenwave and FP-POS independent for a particular grating, but it is grating and stripe dependent. To monitor this effect, we observed selected cenwaves for all NUV gratings.

Execution
The program is comprised of 3 visits of one-orbit each. The wavelength scales of the following settings were monitored in all visits: G185M/2010, G225M/2217, G285M/2676, and G230L/2635/2950/3000 (all at FP- POS=3). External target HD6655 was used, as in previous cycles. V01 and V03 executed successfully on January 2nd, and September 2nd, 2014. In V02, (May 1st), the target acquisition sequence moved the target away from the center of the COS aperture by about +1 arcsec in the cross-dispersion direction causing significant vignetting. The mis-centering was traced back to a bad pair of guide stars. The data in V02 were therefore not usable for checking the dispersion solution zero-point in the May timeframe.

Summary of Analysis and Results
For spectra that overlap with STIS E230M data of HD6655, offsets between the COS and STIS ISM lines were measured for each setting using a cross-correlation analysis. These offsets are listed in Table 1 in units of pixel. For those settings that have no overlap with the STIS E230M data, offsets were measured relative to the same epoch of Cycle 19 COS monitoring program 12722. These offsets are listed in Table 2.

Accuracy Achieved
The COS specifications for NUV wavelength accuracies are 1.7 – 2.4 pix for G185M, 2.3 – 3.2 pix for G225M, 2.3 – 3.5 pix for G285M, and 2.0 – 3.7 pix for G230L. The results given in Table 3 seem to indicate that there is a systematic offset, of +1.3 to ~ +5 pix between the zero point of the COS/NUV and STIS/E230M wavelength scales. When comparing the Cycle 21 data with Cycle 19 data taken at a similar epoch (Table 4), there are small variations of the zero point of the COS wavelength scale, which are within the accuracies given above. The required accuracy is achieved within errors (0.5 pixels) in all cases.

Reference Files Delivered
N/A

Relevant ISRs
Details are included in the Cycle 21 close-out summary and in a multi-cycle comparison ISR (Sonnentrucker et al. 2015, in prep)

Continuation Plans
This program is continued in Cycle 22 under PID 13975. Three monitoring visits of 1 orbit each were scheduled to execute every ~4 months.

Supporting Details

Table 3. Offsets in pixels that need to be applied to shift the COS/NUV spectral lines of HD 6655 so that they align with the STIS E230M spectral lines (reference) of the same target. For G230L spectra, stripe C contains mostly second order light. Stripe A covers wavelengths shorter than ~ 2100 Å. For both of these stripes there is no overlap with the wavelength range of the STIS E230M data. The same applies to stripes A and B of G225M/2217 and all the stripes of G185M/2010.

Visit	Stripe	G225M 2217	G285M 2676	G230L 2635	G230L 2950	G230L 3000
Jan. 2	A B C	... … +5.1	+3.4 +2.5 +3.6	… +2.4 …	… +3.9 …	… +2.2 …
Sept. 2	A B C	... … +5.0	+2.6 +1.9 +2.4	… +1.6 …	… +3.0 …	… +1.3 …

Table 4. Offsets in pixels between the Cycle 21 COS/NUV spectra of HD 6655 and the Cycle 19 COS/NUV spectra (PID12722) taken at similar epochs for all settings with adequate S/N ratios.

Visit	Stripe	G185M 2010	G225M 2217	G285M 2676	G230L 2635	G230L 2950	G230L 3000
Jan 2	A B C	... +1.9 +2.3	+1.7 +1.8 +1.5	+1.4 +1.2 +1.6	… +1.7 …	… +1.5 …	… +2.1 …
Sept. 2	A B C	... +1.6 +2.0	+0.8 +1.4 +2.2	+0.9 +1.3 +1.2	… +1.3 …	… +1.2 …	… +1.2 …

Proposal ID 13526: Monitoring of ACQ/IMAGE performance

(PI: Steven Penton)

Analysis Lead, Others: Steven Penton

Summary of Goals and program design

This program was designed to check several parameters related to COS target acquisition (TA). The first goal was to test the co-alignment of the four COS ACQ/IMAGE modes (PSA+MIRRORA, PSA+MIRRORB, BOA+MIRRORA, and BOA+MIRRORB). The second goal was to check the "WCA-to-PSA" and "WCA-to-BOA" offsets for all COS NUV and FUV gratings. The third goal is to test the effects of gain sag on PEAKXD (LTAPKXD) spectroscopic TAs at the current lifetime position.

The co-alignment of PSA+MIRRORA and PSA+MIRRORB is actually obtained in a separate program (13616). This program (HST Cycle 21 Focal Plane Calibration (SI-FGS Alignment, PI=Cox), executes every six months as a part of the Science Instrument (SI) to Fine Guidance Sensor (FGS) alignment check.

Program 13526 consists of three visits. The first visit begins with a co-alignment check of PSA+MIRRORB to BOA+MIRRORA ACQ/Images. After this check, the WCA-to-PSA offsets are checked for G230L/2950, G285M/2850, G130M/1309, and G140L/1280. The second visit was executed on a second, brighter, target, This visit begins with a co-alignment check of the BOA+MIRRORA to BOA+MIRRORB ACQ/Images. After this imaging alignment check, the WCA-to-PSA offsets were checked for G185M/1890, G225M/2306, and G160M/1600. The measurement of the WCA-to-BOA offset for G160M/1623, was dropped from the Cycle 20 equivalent program (13124) in favor of a gain-sag test. Two G160M/1600 spectra were taken in the cross-dipersion direction (XD) by ±0.7". All spectroscopic exposures were taken of FPPOS=3, as this is the FPPOS used during target acquisition. At the end of Visit 02, four WCA lamp only images were obtained as a 'family portrait' of the WCA images for the four ACQ/IMAGE grating/mirror combinations. As these are internal exposures, this did not increase the number of orbits for this program.

A third visit of 13526 was prepared as a contingency visit in the case of a problem with the execution of Visit 02 of 13616, but it was not executed. However, a problem was discovered with MIRRORB ACQ/IMAGE TAs. This contingency visit was re-purposed to verify that the changes that we implemented to correct the MIRRORB ACQ/IMAGEs were successful.

Execution

Visit 02 of 13616 executed on Oct 27, 2104. Visit 01 of 13526 executed on Nov. 19, 2014 and Visit 02 of 13124 executed on Nov 17, 2014. Visit 03 (the contingency visit) executed on October 6, 2014. Note that the contingency visit went first so that MIRRORB ACQ/IMAGEs could be re-certified. Once re-certified, MIRRORB ACQ/IMAGEs were once again available for testing in Visits 01 and 02. All observations were successful.

Summary of Analysis and Results

The ACQ/Images showed that the imaging TA modes were co-aligned to about 1.6 NUV pixels in AD which equates to about 0.04". This is larger than expected as in SMOV, these channels were co-aligned to better than 0.5 pixels (0.01"). The strictest NUV TA AD accuracy requirement is for the G185M, which is 0.058", the strictest FUV centering TA requirement is for G130M, which is 0.150". In XD, the modes were off by as much as 4.5p

(0.105”). The XD requirement is 0.3”, but the goal is 0.1”. These offsets are close to our centering requirements, and further investigation is warranted.

Drift analysis of the OSMs shows that both OSM1 and OSM2 are drifting. OSM1 is drifting in the +AD, while OSM2 is drifting in the –AD. There has also been increased scatter in both AD and XD. This unpredictable drift scatter is likely the reason for the measured AD & XD offsets described above. No adjustments were made to the ACQ/Image MIRRORB WCA-to-PSA/BOA offsets based upon the data of this program. If the Cycle 22 equivalent program shows similar results, a special calibration program may be required to re-derive the NUV imaging WCA-to-SA offsets.

Based upon the data of 13526, the WCA-to-SA offsets for the NUV or FUV gratings were not changed, even though some of the offsets appeared to have changed slightly from previous measurements. In other words, it was not possible to untangle XD pointing error from an actual change to the WCA-to-SA offsets. The uncertainty of why the BOA ACQ/Image modes were not co-aligned precluded the use of this data for these purposes.

Accuracy Achieved

Imaging WCA-to-SA offsets need to be known to better than 0.5 NUV pixels in both dispersion and cross- dispersion (XD). Spectroscopic WCA-to-SA offsets need to known to 0.5 XD pixel. These goals were not achieved with the data of this program.

Reference Files Delivered

No reference files were delivered.

Relevant ISRs

No ISRs were produced from this program, but this data should be combined with the Cycle 20 and Cycle 22 programs for a possible TIR documenting any NUV imaging re-alignment.

Continuation Plans

This program is to be continued annually, with the Cycle 22 program being 13972.

Proposal ID 13521: COS/FUV Detector Dark Monitor

(PI: Justin Ely)

Analysis Lead, Others: Justin Ely, David Sahnow

Summary of Goals and program design

Perform routine monitoring of FUV XDL detector dark rate. The main purpose is to look for evidence of a change in the dark rate, both to track on-orbit time dependence and to check for a developing detector problem. Results from this program are used to update the ETC.

Execution

Every week, five 22-minute exposures were taken with the shutter closed for a total of 260 orbits. All observations were successful.

Summary of Analysis and Results

After screening for SAA passages, the dark rate of each observation was measured in 25 second intervals from a region that excluded the noisy edges of the active area. Dark rates were measured vs. time and summed darks for each visit were constructed from all non- SAA impacted events.

The overall trend in the dark rate has been relatively constant for Segment B, while Segment A appears to have again experienced a persistent baseline increase in mid 2014. The baseline jump exhibits similar behavior to past occurrences: an initial discontinuous increase followed by a slow, many-week, decrease back to nominal (Figure 5).

Additionally, both segments show individual observations and portions of observations that significantly vary from the baseline dark rate. Both of these effects appear to have some correlation with the solar cycle, though direct cause and effect have not yet been determined.

Accuracy Achieved

Due to the lack of a measureable trend and the extreme variability seen in observations, we adopt an ETC estimate for the dark-rate that corresponds to the 95% level in the probability distribution function determined from dark measurements over a period of the previous 6 months – 1 year.

Reference Files Delivered

None

Relevant ISRs

None

Continuation Plans

Program continued in Cycle 22 as 13967.

Supporting Details

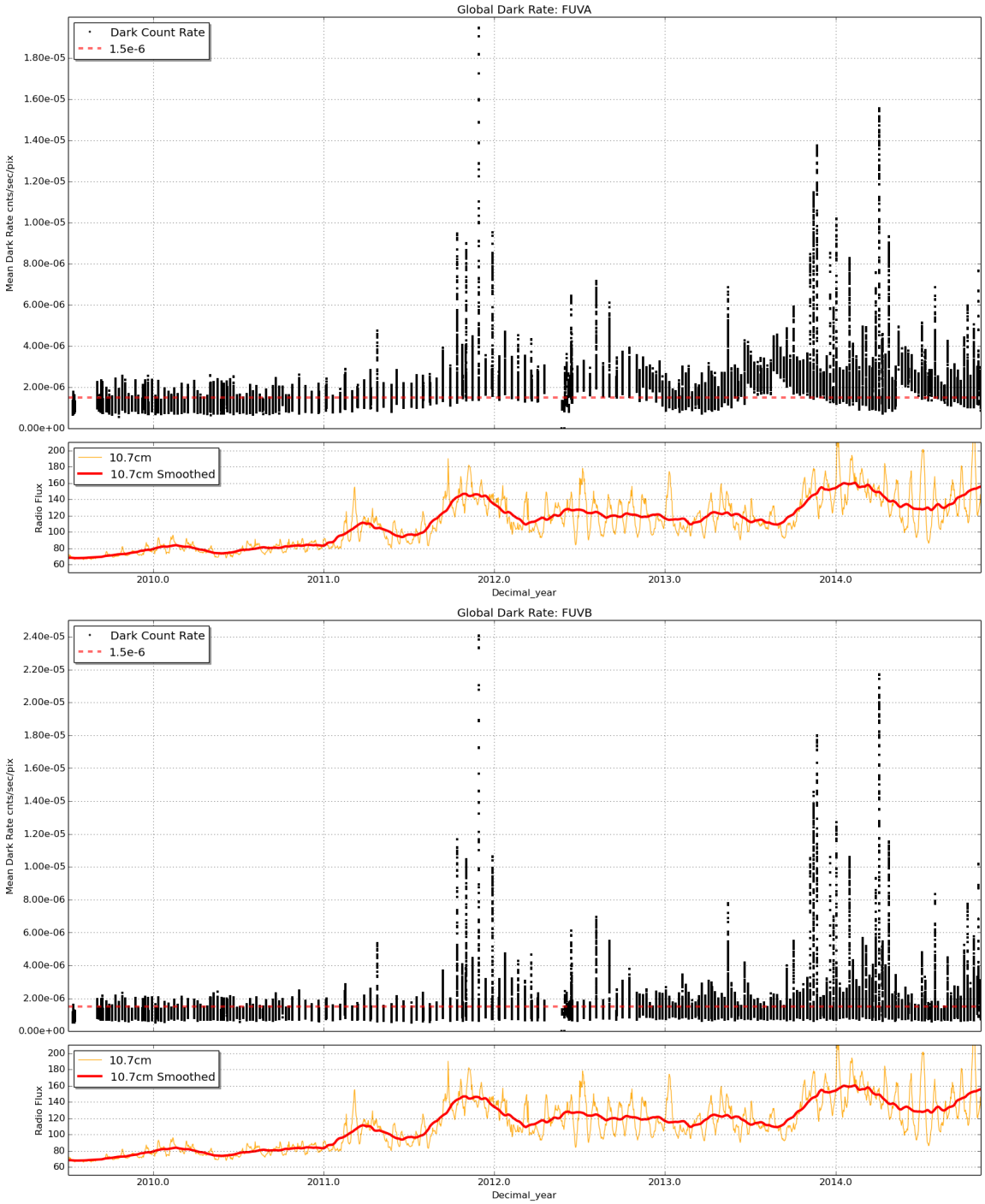

Figure 5. COS/FUV dark rates on FUVA (top) and FUVB (bottom) as a function of time, from COS installation through Cycle 21. The first subplot shows the measured dark-rate in 25 second increments throughout every observation. The groupings of points represent individual visits, and demonstrate that the variability within a given exposure is sometimes extremely large. The red dashed line displays a fiducial dark rate of 1.5×10-6 cts/pix/s. The bottom panels display the 10.7 cm emission tracking the solar cycle.

Proposal ID 13520: COS FUV Time-Dependent Sensitivity

(PI: K. Azalee Bostroem)

Analysis Lead, Others: Hugues Sana

Summary of Goals and program design

Monitor the sensitivity of each FUV grating to detect changes due to contamination or other causes. Characterize these changes as a function of wavelength, grating, and segment, and update the time-dependent sensitivity reference file, if necessary, for use with pipeline flux calibration. Exposure times are set to obtain a signal to noise ratio (S/N) of 15 at the wavelength of *least* sensitivity except for modes G130M/1055, G130M/1096, G140L/1055, and G140L/1280 where the sensitivity falls off steeply towards shorter wavelengths. Exposure times for the G130M/1055 and 1222 are chosen to reach a S/N of 25 at the wavelength of *most* sensitivity.

Two white dwarf standard stars are used to monitor the FUV TDS in Cycle 21: WD0308-565 and GD71. The target used to monitor each mode is detailed in Table 5 and are chosen to optimize the S/N of the mode while minimizing the impact of the monitoring on the detector lifetime.

There are no wavelength calibration lamp lines available on the wavelength range covered by G130M/1096/FUVB. Visits include a lamp observation with FUVA taken after the science observation with FUVB and before any OSM movement.

Table 5. Targets used to monitor different COS FUV modes

Grating	Central Wavelength	FUVA Target	FUVB Target
G130M	1055	WD0308-565	WD0308-565
	1096	GD71	GD71
	1222	WD0308-565	WD0308-565
	1291	WD0308-565	WD0308-565
	1327	WD0308-565	WD0308-565
G160M	1577	GD71	WD0308-565
	1623	GD71	WD0308-565
G140L	1105	WD0308-565	WD0308-565
	1230	WD0308-565	WD0308-565

Execution

The acqusition strategy of the last two visits with target GD71 (visits 29 and 31; Aug and Sept 2014) was modified (from MIRRORB to dispersed ACQ) following issues with MIRRORB acquistions. The exposure order was reshuffled (first G130M, then G130M to allow the program to still fit within a single orbit. Bookkeeping: August visit: initially labelled 29, the visit was withdrawn and replaced by visit 99; September: the initial label (31) was kept but the visit structure was updated before execution following the modified acquisition strategy described above.

Summary of Analysis and Results

All observations were analyzed using the *cos_tds_analysis.py* script as described in Bostroem (COS TIR 2014-05). The net counts spectrum is binned into 5/20 Å bins for the medium/low resolution modes, respectively. The data taken with the present set of targets (WD0308-565 and GD71) are scaled to match the original targets using the data from program 12806. A trend is fit to LP1 and scaled LP2 data and the final relation is scaled such that the fit is 1 at May 01, 2009 (MJD=54952.0). The analysis uses breakpoints of 2010.2, 2011.2, 2011.75, 2012.0, 2012.8 and 2013.8. The latter breakpoint has been newly introduced to account for increased slopes compared to previous cycle. A summary plot of the sensitivity vs. time for each segment and solar activity directed towards Earth (Figure 6; created using the *make_solar_cycle_plot.py* script).

Slopes for Cycle 21 are increased compared to last cycle; and reach up to about -7%/yr for FUVA. The increased downwards trends coincide with enhanced solar activity. These trends are summarized in Table 6 and Figure 7.

A new TDS reference file was delivered in December 2014 where the increased slope after 2013.8 are taken into account.

Table 6. COS FUV TDS trends for each grating and segment. The values shown are the maximum and minimum values for all central wavelengths observed with a given grating during Cycles 20 and 21.

	Cycle 20		Cycle 21	
Grating	**Slope FUVA**	**Slope FUVB**	**Slope FUVA**	**Slope FUVB**
G130M	-5.1 – +0.4	-0.9 – +2.1	-6.8 – -1.7	-2.0 – +1.1
G160M	-3.1 – +0.1	-1.3 – +2.9	-6.1 – -3.0	-3.2 – +0.2
G140L	-3.3 – +3.7	-0.5	-6.1 – +1.1	-0.4

Accuracy Achieved

For the standard modes a S/N of 15 at the wavelength of least sensitivity is reached with the exception of G140L FUVA whose sensitivity is extremely low at the long wavelength edge. For G140L FUVA the S/N < 15 for wavelengths greater than 1840 Å. The blue modes (1096 and 1222) achieve the required signal to noise ratio of 25 at the wavelength of most sensitivity.

Reference Files Delivered

ycj1846tl_tds.fits

Relevant ISRs

None

Continuation Plans

This program continued in Cycle 22 as program 13967. The monitoring is kept identical, with the exception of an additional complete visit in order to perform the TDS reconnection across lifetime positions 2 and 3 (lifetime position change on February 2015).

Supporting Details

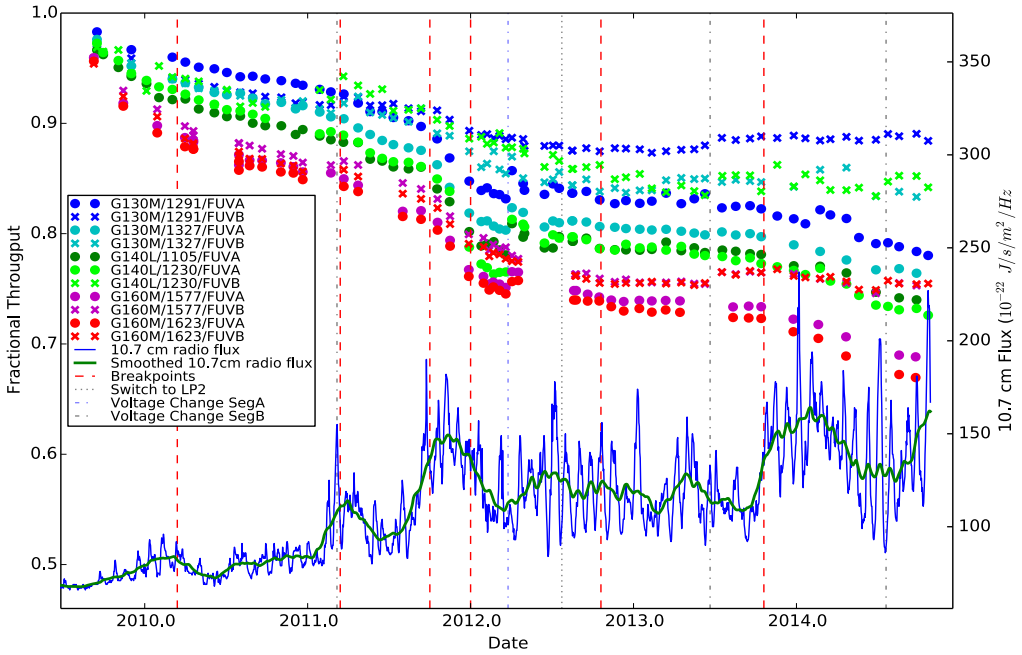

Figure 6. Decline of the COS FUV spectroscopic sensitivity over time (symbols) compared to the solar activity directed at Earth as tracked by 10.7 cm flux (blue solid lines; smoothed as shown by the green line). The dashed red vertical lines represent breakpoints in the piece-wise function used to model the TDS. The dotted grey vertical line marks the move to lifetime position 2 (and the new targets), and the dot-dashed grey vertical lines correspond to changes in the operational voltage.

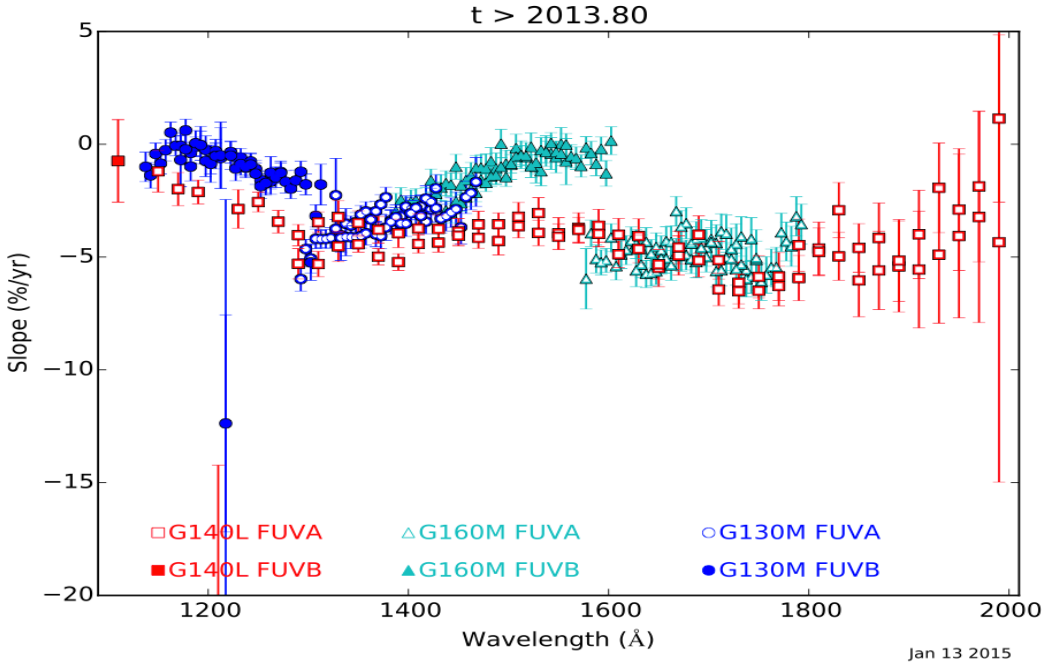

Figure 7. COS FUV TDS slope during Cycle 21, expressed in percent per year and plotted as a function of wavelength for the different gratings (see legend). FUVA is plotted as open symbols and FUVB as closed symbols. G130M is represented with blue circles, G160M with cyan triangles, and G140L with red squares. The variation in trend from segment to segment within a grating is apparent.

Proposal ID 13522: COS FUV Internal/External Wavelength Scale Monitor (PI: Paule Sonnentrucker)

Analysis Lead, Others: Paule Sonnentrucker

Summary of Goals and program design
This program monitors the offset between the internal and external wavelength scales. This offset is referred to as "DELTA" in the wavelength dispersion solution reference file and corrects for the shift between the WCA and PSA in TV03 versus the shift between the WCA and PSA on orbit: $(WCA - PSA)_{TV03}$ - $(WCA - PSA)_{orbit}$. Analysis of TV data indicate that this DELTA (offset) is cenwave and FPPOS independent for a particular grating, but it is grating dependent. To monitor this effect, this calibration program observes some cenwaves at different FP-POS positions for all gratings.

Execution
This program is comprised of one visit of 3 orbits to monitor the wavelength scales of the G130M, G160M and G140L gratings using the external SMC target AV75. V01 executed successfully on March 15, 2014. All cenwaves for G140L and the extreme cenwaves for G130M and G160M were observed. Alternate FP-POS positions were used for the M gratings to mitigate gain-sag effects. FP-POS=3 was used for G140L.

Summary of Analysis and Results
Archival STIS E140M data were used to perform a cross-correlation analysis against the COS G130M, G160M and G140L data following the procedure described in Sonnentrucker et al. 2013 (ISR 2013-06). The offsets, in pixel, of the COS ISM lines relative to the STIS E140M data resulting from the cross-correlation analysis are reported in Table 7 and displayed in **Figure 8**.

Accuracy Achieved
The offsets measured are within the 1σ error goals for the COS/FUV wavelength scales, of 5.7-7.5 pix for G130M, 5.8-7.2 pix for G160M, and 7.5-12.5 pix for G140L (see Oliveira et al. 2010, ISR 2010-06)

Reference Files Delivered: N/A

Relevant ISRs
Results are reported in the Cycle 21 close-out summary and will be added to a multi-cycle ISR comparison (Sonnentrucker et al. 2015, in prep)

Continuation Plans
This program is continued in Cycle 22 under PID 13969 for a total of 1 orbit. This program covers only the G130M/1096 and G140L/1105 &1280 configurations. Monitoring of the other standard COS/FUV configurations will be done using data from LCAL2 program 13931, as part of the calibration of Lifetime position 3 (LP3).

Supporting Details

Table 7. Offset range returned by cross-correlating the COS 1xdsum spectra with the archive STIS E140M/1425 data using observations from external SMC target AV75

Target	Grating	Offset range (pixel)
AV75	G130M	-5.3, +4.1
AV75	G160M	-6.5, +2.6
AV75	G140L-1280	-3.9, +3.8
AV75	G140L-1105	-4.9, +4.1

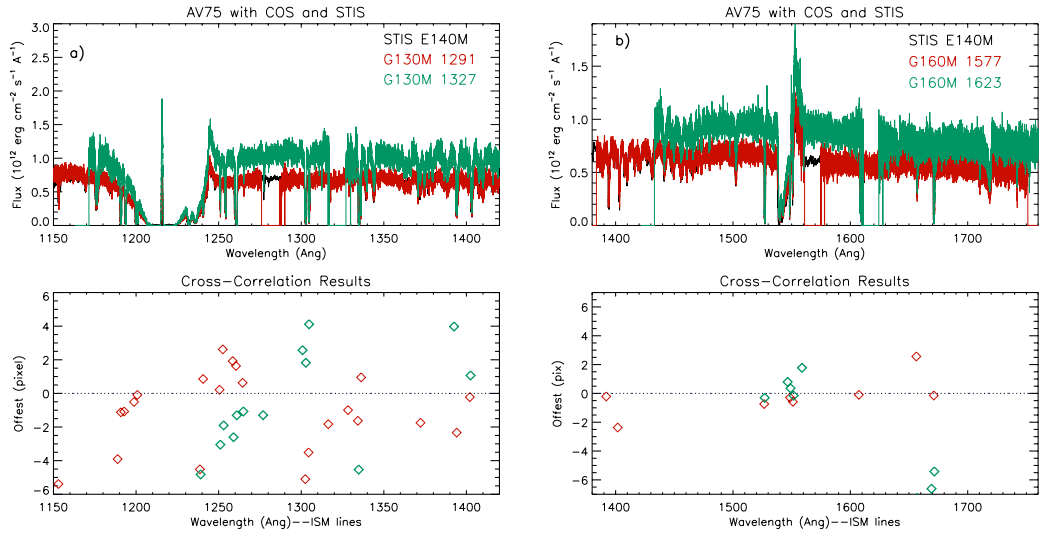

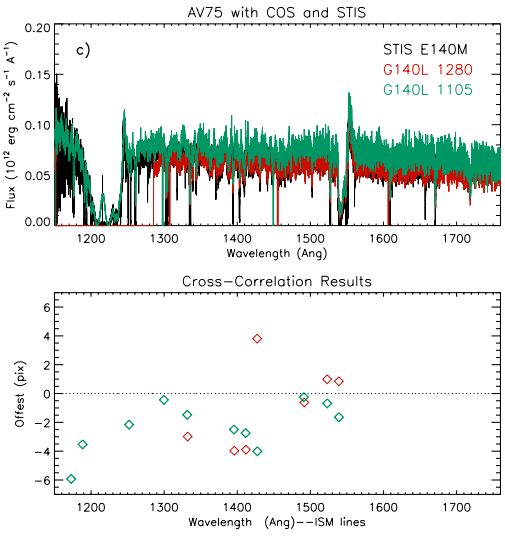

Figure 8a. *Top*: Spectra of AV75 obtained with the STIS E140M/1425 mode (black), the COS G130M/1291 mode (red) and the COS G130M/1327 mode (green). The G130M/1327 data are displaced in Y for clarity. *Bottom*: Offset in pixels measured between ISM lines in the STIS E140M and G130M/1291 spectra (red) and the STIS E140M and G130M/1327 spectra (green).

Figure 8b. *Top*: Spectra of AV75 obtained with the STIS E140M/1425 mode (black), the COS G160M/1577 mode (red) and the COS G160M/1623 mode (green). The G160M/1623 data are displaced in Y for clarity. *Bottom*: Offset in pixels measured between ISM lines in the STIS E140M and G160M/1577 spectra (red) and the STIS E140M and G160M/1623 spectra (green).

Figure 8**c.** *Top*: Spectra of AV75 obtained with the STIS E140M/1425 mode (black), the COS G140L/1280 mode (red) and COS G140L/1105 mode (green). The G140L/1105 data are displaced in Y for clarity. *Bottom*: Offset in pixels measured between ISM lines in the STIS E140M and COS G140L/1280 spectra (red) and the STIS E140M and G140L/1105 spectra (green).

Proposal ID 13525: COS FUV Detector Gain Maps

(PI: David Sahnow)

Analysis Lead, Others: David Sahnow

Summary of Goals and program design

This program uses the deuterium lamp to illuminate the entire LP2 region of the detector. The pulse height information obtained is then used to create gain maps which are used to monitor gain sag.

Execution

Visits 01 and 02 executed immediately before and after the High Voltage (HV) on Segment B was changed on 7/21/2014. Visits 11 and 12 executed immediately before and after the HV on Segment A was changed on 11/3/2014. All four visits ran as expected.

Summary of Analysis and Results

The standard gain map creation routines were used to measure the modal gain in the illuminated region.

Accuracy Achieved

The modal gain is typically measured to ~0.1 Pulse Height bins.

Reference Files Delivered

The data from this program, along with data from other exposures, is used in construction of the GSAGTAB.

Relevant ISRs

None.

Continuation Plans

This program continued in Cycle 22 as Program 13970. Two major changes were made for that program: (1) two cross-dispersion locations were used in each visit in order to sample the full extent of the PSF; and (2) data was taken at the HV being used for G130M/1222.

Supporting Details: None

Proposal ID 13548: COS Observations of Geocoronal Lyman-alpha Emission
COS Pure Parallel
(PI: Hugues Sana)

Analysis Lead, Others: Sean Lockwood

Summary of Goals and program design

Whenever possible, obtain parallel airglow spectra with COS. Data this cycle were taken at lifetime position 3 in the G130M/c1327 mode at all four FP-POS. Dataset names are listed on the STIS airglow website, but no analysis of the data is performed.

Execution: See Table 8

Table 8. Overview of the execution of the COS Geocoronal Lyman-alpha emission program

Visit	ASN_ID	IPPSSOOT	Mode	Exptime
E1[a]	LCETE1060	LCETE1WDQ	G130M/1327/+0/LP2	2900 s
E2	LCETE2060	LCETE2HXQ	G130M/1327/-2/LP2	2900 s
E3	LCETE3060	LCETE2Q8Q	G130M/1327/+1/LP2	2900 s
E4	LCETE4060	LCETE4R8Q	G130M/1327/-1/LP2	2900 s
E5[b]	LCETE5060	LCETE5J6Q	G130M/1327/-1/LP2	2900 s

a. STIS observations failed, b. Repeat of E1

While all observations were taken, LCETE2060 in visit E2 truncated early at 2272 s instead of 2900 s for unknown reasons.

Summary of Analysis and Results
The goal of 10,000 s exptime for G130M/c1327 at lifetime position 2 has been achieved.

Total exposure time: 13,872 s
Total counts within PSA FUVA: 26,298
Total counts within PSA FUVB: 4,362,763
Total counts within PSA both: 4,389,061

Dataset names have been added to the COS Airglow website:
http://www.stsci.edu/hst/cos/calibration/airglow.html

Accuracy Achieved
No analysis was performed.
(Desired accuracy: For G130M, SNR of 2 per pixel at 1213 A.)

Relevant ISRs

Continuation Plans
Continue observations in Cycle 22 by taking geocoronal observations with G130M/c1291 at lifetime position 3.

Supporting Details: None

Proposal ID 13523: COS Pt-Ne Lamp Cross-Calibration

(PI: Steven Penton)

Analysis Lead, Others: Steven Penton

COS carries two Platinum-Neon (PtNe) hallow cathode lamps used for wavelength calibration and aperture location during target acquisition (TA). Each lamp contains 3 current settings (LOW, MEDIUM, & HIGH), with the only common setting on both lamps being medium current (10 mill-amps, mA). Each lamp is expected to last 800-1000 hours of medium usage (8-10 Amp-Hours, A-h). PtNe#1 is currently used for the TAGFLASH wavelength calibration exposures for all COS science exposures, while PtNe#2 is used during spectroscopic (PEAKXD) and imaging (ACQ/IMAGE) target acquisitions (TAs). As of August, 2015, PtNe#1 has been used ~3 A-h, and PtNe#2 about ~1 A-h.

This program is designed to cross-calibrate the lamps, so that the required exposure times for both lamps are known for all uses (TAGFLASH and TA). This will allow us to resume standard science operations as quickly as possible should one of the Pt-Ne lamps fail.

Summary of Goals and program design

The goals of this program are

1. Ensure that the current TAGFLASH times, for COS PtNe#1 are still valid as of January 2015. Provide an update to these times, if required.
2. Provide a ratio of PtNe#1 to PtNe#2 at medium current, 10 milli-amps, as a function of wavelength for the entire COS bandpass
3. Create a TAGFLASH exposure time table for the COS PtNe#2 wavelength calibration lamp.
4. Provide a TA exposure time table (imaging and spectroscopic) for PtNe#1.

One PSA/MIRRORB PtNe #1/Low current lamp exposure is used to calibrate TA in time-tag imaging mode. Internal PtNe#1 and #2 lamp time-tag spectra at medium current are obtained to cross-calibrate the lamps, determine any changes to the PtNe#1 lamp spectrum and derive PtNe #2 TAGFLASH times. The FUV will be covered by a single FUV/G140L/1105 spectrum and the NUV by three overlapping G230L exposures (2635, 3000, and 3360 central wavelength settings).

Recent COS NUV lamp images shows that PtNe #2 lamp at its low current setting produces ~15.2 counts/s in PSA/MIRRORB mode. Ground testing indicates that PtNe #1 lamp is ~5.5x brighter at its low current, or 84 counts/s. The WCA/WAVECAL image is 5x12 pixels, so the brightest pixel is ~ 1 ct/s, well below the safety screening limit of 50 cts/s. The MIRRORA to MIRRORB ratio is ~20, so there is also no safety issue with low current PtNe#1 WCA images.

Execution:

This one-orbit program executed as expected on Nov 11, 2013.

Summary of Analysis and Results

In general it appears that PtNe#1 is about 10% brighter than PtNe#2, except at the low (<1500 Å) and high (>3000 Å) wavelength edges, where it is ~20% brighter. Some aging of the PtNe#1 lamp is present and it appears likely than some changes will be recommended to the existing TAGFLASH times.

Accuracy Achieved

The spectra are of sufficient quality to determine updated exposure times for both lamps for both TA and TAGFLASH usage.

Reference Files Delivered

No reference files will been delivered, but updated TAGFLASH and PEAKXD exposure time tables are in preparation.

Relevant ISRs

An ISR is in preparation for this program.

Continuation Plans

No follow-up observations are required, however, spot-checking should be performed in the event of a side switch or lamp failure.

Proposal ID 13530: NUV Focus Sweep

(PI: David Sahnow)

Analysis Lead, Others: David Sahnow

Summary of Goals and program design

This program performs an NUV focus sweep in order to determine whether the COS focus has changed since it was originally measured in Program 11469 during SMOV. Nineteen 60 second exposures of NGC188-41 were taken during a single orbit with OSM1 moved over the range from -200 to +200 steps.

Execution

The program was executed on December 5, 2013, and it worked as expected.

Summary of Analysis and Results

The FWHM of each image was measured in both x and y. The commanded OSM1 position along with the time-dependent breathing correction was used to determine the absolute focus position. By plotting FWHM vs. position, the best focus position was determined.

Accuracy Achieved

Although the final analysis has not been completed, the figure below shows that the focus position can be measured to better than ~±30 steps, or ~±1.5 μm. Since the range of the breathing correction is larger than this uncertainty, this is adequate.

Reference Files Delivered

None required.

Relevant ISRs

An ISR with the results of this program and a discussion of other methods to monitor the focus is being drafted.

Continuation Plans

None.

Supporting Details:

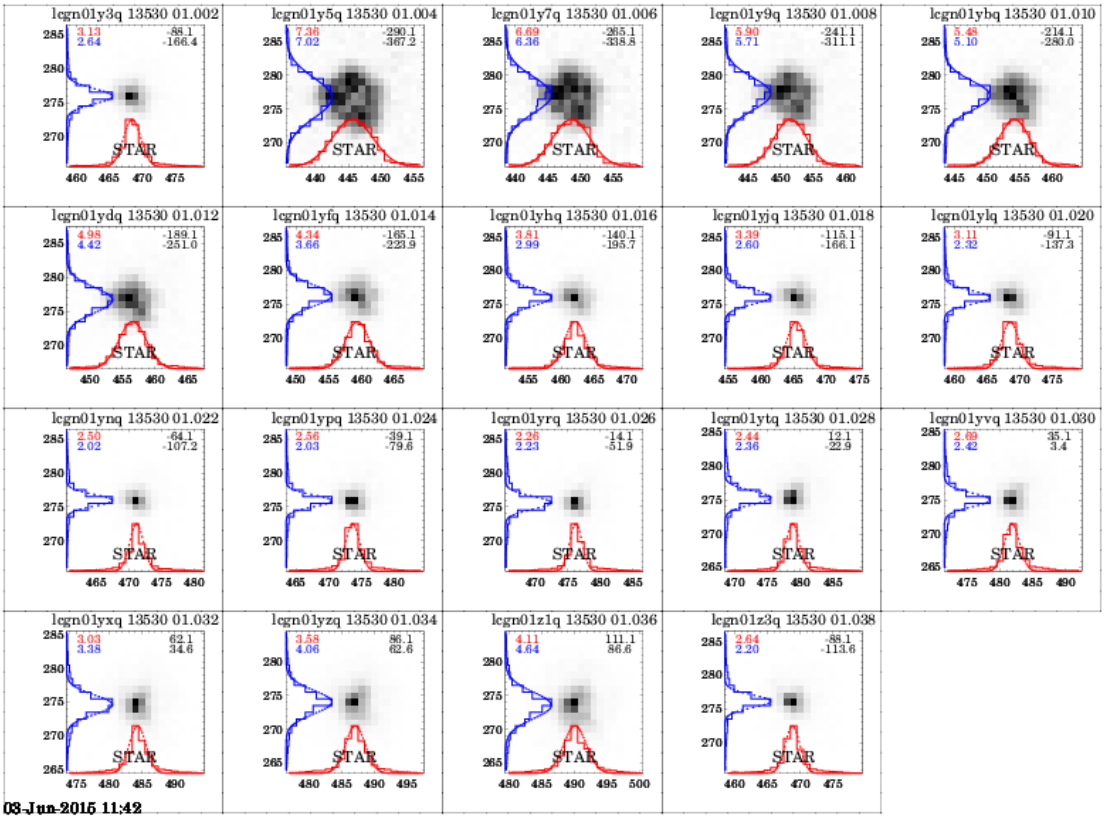

Figure 9 The 19 images taken during Program 13530, arranged in time order from upper left to lower right. The first and last image were taken at the nominal focus, while the ones in between show changes of -200 to +200 focus steps.

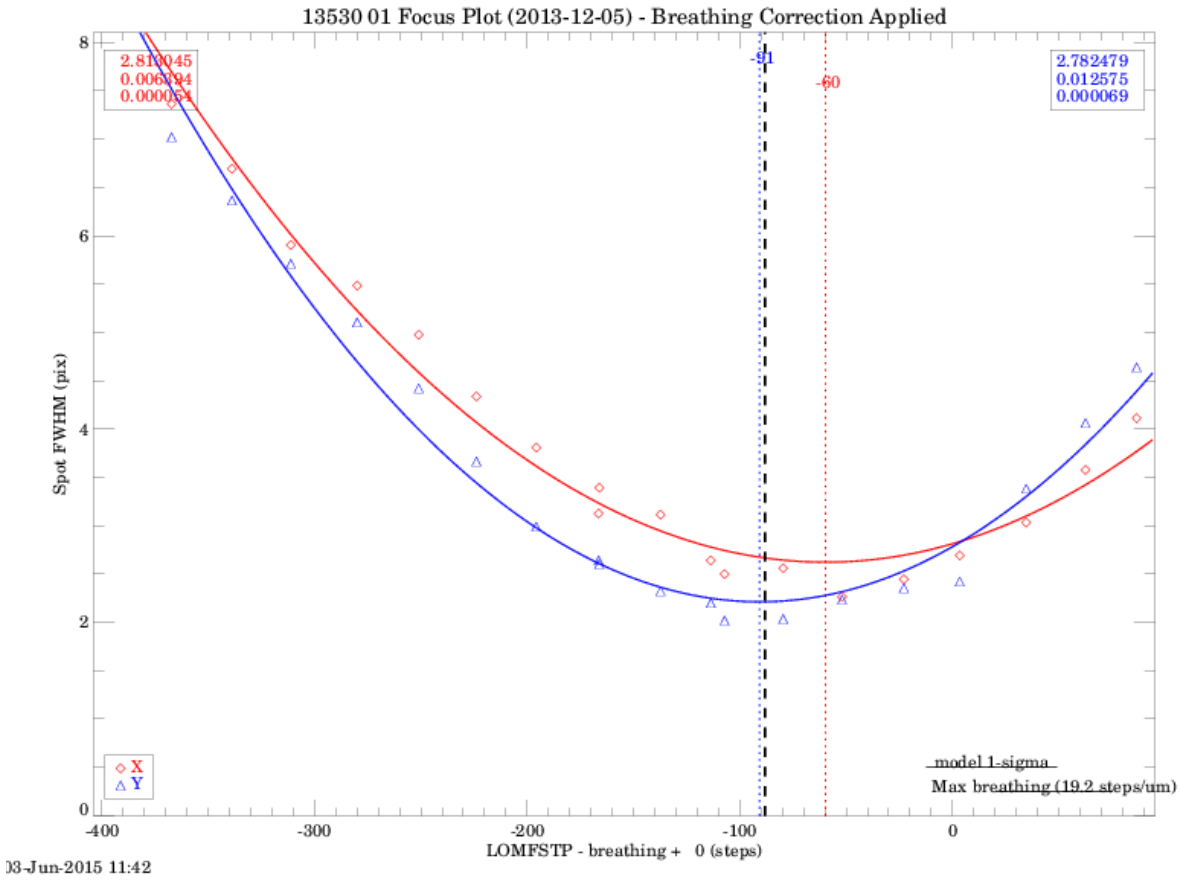

Figure 10 The measured FWHM in the X (red) and Y (blue) directions, using the breathing-corrected focus position.

Appendix

Table 9 lists the COS reference files delivered as part of analysis of data taken in COS Cycle 21 calibration programs.

Table 9. Reference files delivered as a result of the Cycle 21 calibration programs

Reference File	File Type	Delivery Date	Programs Included
ycj1846tl_tds.fits	Time dependent sensitivity (see page 14)	12/19/2014	11897, 12424,12715, 13119, 13520